Available online at www.sciencedirect.com
ScienceDirect
Tetrahedron 63 (2007) 7474–7481
Tetrahedron

Nucleoside-based organogelators: gelation by the G–G base pair formation of alkylsilylated guanosine derivatives

Isao Yoshikawa, Suguru Yanagi, Youhei Yamaji and Koji Araki*

Institute of Industrial Science, University of Tokyo, 4-6-1 Komaba, Meguro-ku, Tokyo 153-8505, Japan

Received 16 November 2006; revised 9 January 2007; accepted 1 February 2007
Available online 8 February 2007

Abstract—2′,3′-*O*-Isopropylideneguanosine derivatives **1a–c** having a bulky alkylsilyl moiety showed excellent gelation ability in alkane solvents. IR spectra of the gel clearly showed the absence of hydrogen bonding interaction at the C(6)═O position and, together with a CD study, a G–G base pair formation by double N(2)H···N(3) and additional N(2)H···O(2′) hydrogen bonds was indicated. X-ray diffraction and SEM studies of the xerogel and AFM observation of the transferred gel suggested the formation of a two-dimensional supramolecular assembly 2 nm in thickness. The G–G base pair formation is discussed in terms of the molecular packing in the two-dimensional assemblies.

1. Introduction

Low molecular mass gelators and their non-covalently bonded supramolecular assemblies have been the subject of continuing interest due to their unique and dynamic properties.[1–4] Nano- to mesoscopic-scale supramolecular assemblies of gelator molecules further developed on the macroscopic scale, three-dimensional structures, and the gelation of solvents are effectively induced at a relatively low concentration. The hydrogen bond is the most frequently used non-covalent interaction for this purpose because of its strong and directional nature. Nucleobases that have multiple hydrogen bond donor and acceptor sites within their molecular structures show high ability to form directionally controlled inter-base hydrogen bond networks,[5] and they have been proven to be excellent low molecular mass gelators.[6]

To understand their gelation ability, the mode of inter-base hydrogen bonding has to be clarified because this is the key to the gelation process. There is a wide variety of hydrogen bonding patterns of nucleobases in crystal structures, i.e., dimer-type base pairs,[7] cyclic oligomers,[8–11] and infinite linear polymers.[12–15] In the case of organogels of guanine (G) derivatives, Gottarelli and his group showed that hydrogen-bonded linear tape I or II[16,17] was responsible for gelation (Fig. 1a and b).[18] In our series of studies on supramolecular assemblies of alkylsilylated nucleoside derivatives,[19–21] we found that the hydrogen-bonded sheet

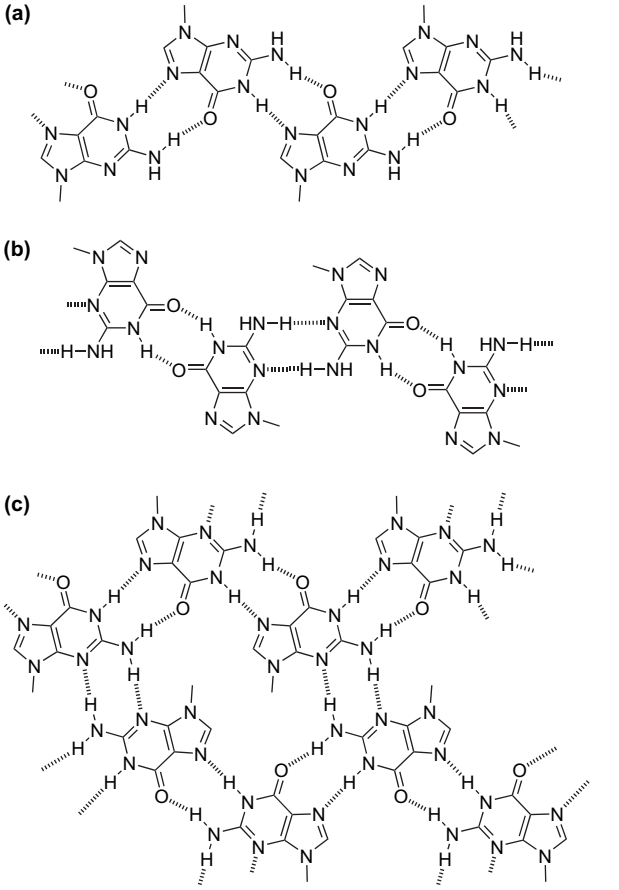

Figure 1. Hydrogen bonding patterns of guanosine derivatives: (a) tape I, (b) tape II, and (c) sheet.

Keywords: Nucleoside; Guanosine; Gelator; Organogel; Hydrogen bond.
* Corresponding author. Tel.: +81 3 5452 6363; fax: +81 3 5452 6364; e-mail: araki@iis.u-tokyo.ac.jp

0040–4020/$ - see front matter © 2007 Elsevier Ltd. All rights reserved.
doi:10.1016/j.tet.2007.02.010

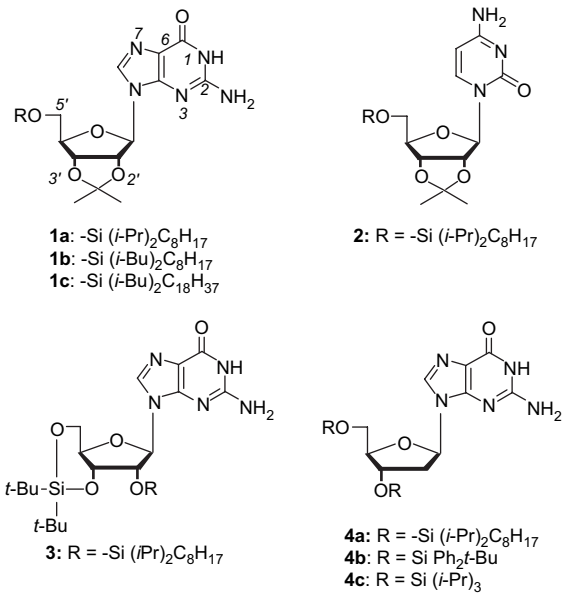

Figure 2. Alkylsilylated nucleoside derivatives.

(Fig. 1c) of alkylsilylated deoxyguanosine derivatives induced gelation of alkane solvents.[22] In this article, we report that 2′,3′-isopropylidene guanosine derivatives **1a–c** show excellent gelation ability in alkane solvents, in which formation of the hydrogen-bonded G–G base pair plays a key role in the gelation process.

2. Results

2.1. Gelation ability

The structures of the alkylsilylated guanosine and deoxyguanosine derivatives, which were synthesized according to the reported procedure,[23,24] are shown in Figure 2. After dissolving these compounds in solvents by heating (5 wt %), the solution was cooled down to room temperature, and their gelation ability was determined by the inversion method.[25] The results are summarized in Table 1. Among the derivatives tested, **1a–c** having the 2′,3′-isopropylidene guanosine structure showed gelation ability in alkane solvents, yielding transparent gels. Though their gelation ability was limited to nonpolar alkane solvents, the minimum concentrations of **1a**, **1b**, and **1c** required for gelation in decane were 0.4 wt % (5×10^{-3} mol dm^{-3}), 0.4 wt % (5×10^{-3} mol dm^{-3}), and 0.9 wt % (9×10^{-3} mol dm^{-3}), respectively, demonstrating their high gelation ability. The alkyl groups of the silyl moiety only slightly affected their gelation ability. Since

Table 1. Gelation ability of **1–3** at 5 wt %

Solvent	1a	1b	1c	2	3
n-Decane	G	G	G	S	P
n-Hexane	G	G	G	S	P
Cyclohexane	G	G	G	S	S
Benzene	S	S	S	S	S
Chloroform	S	S	S	S	S
Acetone	P	P	P	S	P
Ethanol	P	S	S	S	S

G: gel, S: solution, P: precipitation.

Table 2. Gelation ability of **1a**(G) and **2**(C) mixture in dodecane

Molar ratio **1a**:**2**	Concentration of **1a**	
	5 wt %	1 wt %
1:1	S	S
2:1	G[a]	G[a]
10:1	G[b]	N/A

[a] Turbid gel.
[b] Transparent gel.

compound **3**, whose ribose moiety was fixed by 3′–5′ linkage, showed no gelation ability at all, the high gelation ability of **1a–c** could not be ascribed simply to the fixation of ribose puckering by the 2′,3′-isopropylidene linkage. Interestingly, the addition of cytidine derivative **2**, which did not induce gelation by itself, suppressed the gelation ability of **1a** in dodecane (Table 2). Cytosine (C), the counter part of the highly stable Watson–Crick G–C base pair, was quite likely to cause disruption of the inter-guanine hydrogen bonding of **1a**, suggesting the important role of the inter-guanine hydrogen bonds in the gelation process. These results indicated the essential role of both the guanine and the 2′,3′-isopropylidene structures for manifestation of high gelation ability.

2.2. Thermal properties of the 1a/dodecane gel

The thermal properties of the gel were studied by DSC measurement. Figure 3 shows the heating and cooling curves of the **1a**/dodecane gel (5 wt %) in between 30 and 150 °C. Two relatively broad endothermic peaks were observed in the heating curve. Since the corresponding two exothermic peaks appeared in the cooling process, these transitions were reversible. The **1a**/dodecane gel turned into an isotropic liquid above the first endothermic peak at T_1 (peak temperature)=97 °C (heat of transition ΔH_1=1.22 J g^{-1}), showing that this was due to the gel-to-sol transition. Further heating above the second endothermic peak at T_2 (peak temperature)=137 °C (ΔH_2=1.55 J g^{-1}) caused no apparent change and the **1a**/dodecane system remained as an isotropic liquid. Though the heat of the first gel–sol transition ΔH_1 was relatively insensitive to **1a** content in the range of 5–20 wt % (Table 3), that of the second transition ΔH_2 increased as the **1a** content became higher.

Throughout the temperature range from 30 to 150 °C, the **1a**/dodecane system showed no birefringence even at the high

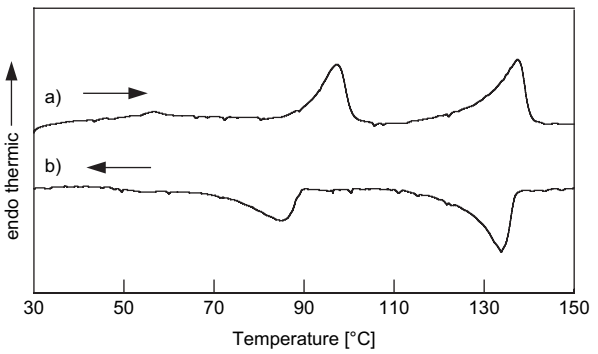

Figure 3. DSC curves of the **1a**/dodecane gel: (a) first heating and (b) cooling curves.

Table 3. Thermal properties of the **1a**/dodecane gel

Concentration of **1a**/wt %	First peak		Second peak	
	T_1[a]/°C	ΔH_1[b]/J g^{-1}	T_2[a]/°C	ΔH_2[b]/J g^{-1}
5	97	1.22	137	1.55
10	98	1.23	141	2.04
20	98	1.15	143	4.61

[a] Peak top.
[b] Including solvent.

1a content (20 wt %). Therefore, **1a** in dodecane was not in an organized structure like the liquid crystals observed for the **4a**/alkane systems.[22]

2.3. Hydrogen bond pattern in the 1a/alkane gel

The mode of hydrogen bonding in the **1a**/dodecane gel was studied by temperature-controlled IR spectroscopy (Fig. 4). The most striking feature of the IR spectrum at room temperature was the sharp C(6)=O stretching peak observed at 1718 cm^{-1} (Fig. 4a). Since the C(6)=O plays a central role in the inter-base hydrogen bonding of guanine derivatives, the peak appears mostly below 1700 cm^{-1} in the solid state because of the hydrogen bond-induced shift to lower energy. In the case of the **1a** powder, the peak appeared at 1695 cm^{-1}. A chloroform solution of **1a** also showed the lower-shifted peak at 1690 cm^{-1} (Fig. 4d). Therefore, the C(6)=O group of **1a** in the solid state or in the chloroform solution was in the hydrogen-bonded state. The **4b** and **4c** crystals, the hydrogen bonding patterns of which were respectively identified to be tape I (Fig. 1a) and sheet (Fig. 1c) by X-ray crystallography,[22] showed peaks at 1701 and 1695 cm^{-1} (Fig. 4e and f). Since the non-hydrogen-bonded C=O stretching of 9-methylguanine in an Ar matrix is reported to appear at 1741 cm^{-1},[26] the results indicated that the C(6)=O group of **1a** was not, or at least was only weakly, hydrogen-bonded in the gel. By increasing the temperature to 80 °C, a lower-shifted peak at 1690 cm^{-1} appeared with a concomitant decrease in the initial peak at 1718 cm^{-1} (Fig. 4b), and the lower-shifted peak became predominant on further heating to 100 °C (Fig. 4c). Therefore, the first endothermic peak at 97 °C observed in the DSC chart was due to the gel-to-sol transition by rearrangement of the hydrogen bonding pattern.

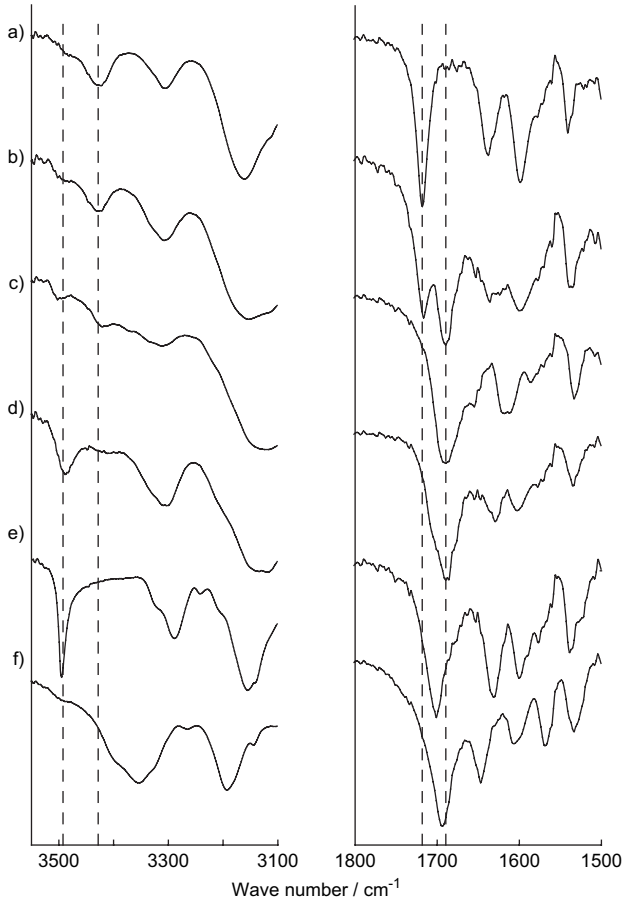

Figure 4. IR spectra of the **1a**/dodecane system (5 wt %) at (a) room temperature, (b) 80 °C, (c) 100 °C, and (d) **1a**/chloroform solution. Those of reference compounds **4b** (e) and **4c** (f) are also shown. Broken lines from the left indicate 3495, 3430, 1720, and 1690 cm^{-1}, respectively.

In the non-hydrogen-bonded NH stretching region from 3400 to 3550 cm^{-1}, the **1a** gel at room temperature showed a band at 3427 cm^{-1}, which decreased by heating to 100 °C, with a weak band then appearing at around 3500 cm^{-1}. To enable the comparison, the NH and CO peak positions of these and other related systems are summarized in Table 4. In chloroform, a band at 3489 cm^{-1} alone was observed. The **4c** crystal, whose N(2)H$_2$ and N(1)H were fully hydrogen-bonded, showed no band in this region, but the **4b** crystal, having the tape I network, showed a sharp peak at 3495 cm^{-1} due to the free NH of the N(2)H$_2$ group. Therefore, in the gel at room temperature, both of the N(2)H$_2$ hydrogen atoms were involved in hydrogen bond formation. Since it has been reported that the non-hydrogen-bonded N(1)H of 9-methylguanine in the amino-oxo form appeared at 3430 cm^{-1},[26] the band observed at 3427 cm^{-1} for the gel at room temperature (Fig. 4a) can be assigned to the free N(1)H stretch. Thus, hydrogen bond formation at the upper rim of the guanine ring, C(6)=O and N(1)H, was indicated to be suppressed in the gel state. These groups only became hydrogen-bonded after transition to the sol state by heating, or in chloroform solution.

Based on these results, the inter-base hydrogen bonding pattern in the **1a**/dodecane gel was considered. Since the C(6)=O and N(1)H groups play major roles in inter-guanine hydrogen bonding, the absence of the hydrogen bonding interaction at these positions suggested that the polymeric hydrogen bonding networks shown in Figure 1 were unlikely to be formed in the gel. Most of the G–G base pairs were also excluded for the same reason, and the G–G base pair formed by the double N(2)H···N(3) hydrogen bonds (Fig. 5) remained as the most probable model. This type of G–G

Table 4. Selected IR peaks of guanine derivatives

	NH$_2$(2) free	NH(1) free	C=O
4b	3493	—	1701
1a/Dodecane, 5 wt %, rt	—	3427	1718
1a/Dodecane 5 wt %, 80 °C	3495	3431	1718,1690
1a/Dodecane 5 wt %, 100 °C	3502	3421	1690
1a/Chloroform, 5 wt %	3489	—	1690
9-Methylguanine[a]	3535, 3435	3430	1741

[a] In an argon matrix.[26]

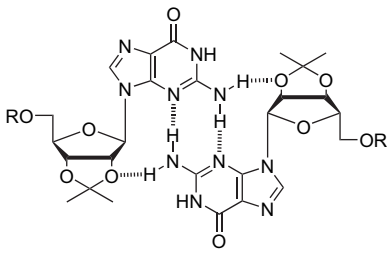

Figure 5. The G–G base pair of **1a–c**.

base pair has been reported for the d(CpG) duplex in acidic conditions.[27,28] Since N(2)H and 2′-O came close to each other in this model, hydrogen bond formation between these groups explained the absence of the free NH band of the $N(2)H_2$ group at around 3500 cm^{-1}, and the necessity of the 2′,3′-isopropylidene structure for gelation.

This G–G base pair formation is further supported by circular dichroism (CD) spectroscopy (Fig. 6b). Though the CD band of the **1a**/chloroform solution was negligibly weak, the **1a**/cyclohexane solution (1.0×10^{-4} M) showed a clear positive CD in the guanine B_{2u} transition band at around 275 nm.[29] Because of the high concentration of **1a** in the gel, no quantitative CD spectra of the gel could be measured. Instead, qualitative CD spectra were recorded by sandwiching the **1a** gel between two flat quartz plates, which showed a similar positive CD band in the same region. Therefore, the observed CD signal in the cyclohexane solution must represent the hydrogen-bonded **1a** in the gel. Since the CD band was observed in the guanine absorption region, rotation along the *N*–glycosyl (N_9–$C_{1'}$) bond was restricted in order to fix the spatial arrangement of the guanine and the ribose

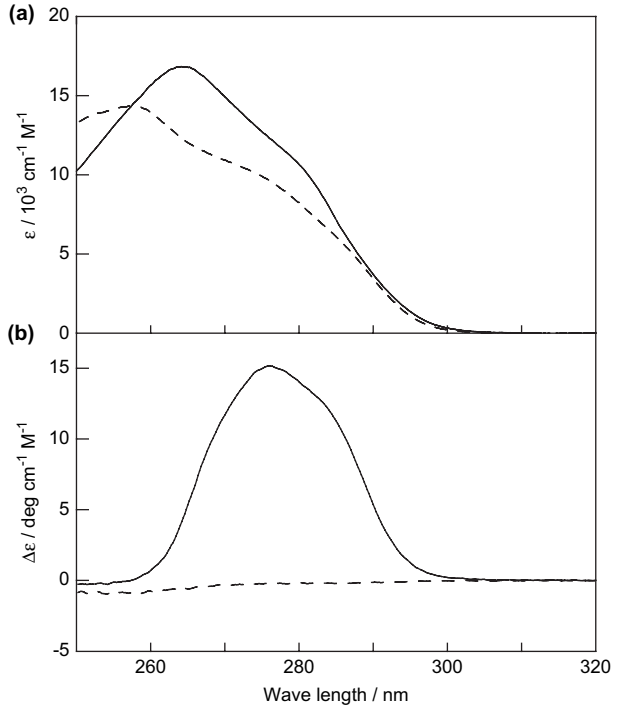

Figure 6. (a) Electronic absorption and (b) CD spectra of **1a** (1×10^{-4} mol dm^{-3}) in cyclohexane (solid line) and chloroform (dashed line).

units. Therefore, this result strongly supports the presence of the N(2)H and 2′-O hydrogen bond to fix the *N*–glycosyl bond rotation. The observed positive CD at the B_{2u} band is suggestive of the *anti* conformation of **1a** around the glycosyl bond in the gel,[30] further supporting this G–G base pair model. Thus, it is concluded that the hydrogen bonding pattern of **1a** is the G–G base pair shown in Figure 5, which is responsible for gelation.

2.4. Structures of the supramolecular assemblies in the 1a/dodecane gel

The structures of the mesoscopic-scale supramolecular assemblies in the **1a** gel were studied by X-ray diffraction (XRD), scanning electron microscopy (SEM), and atomic force microscopy (AFM). Figure 7 shows an SEM image of the xerogel prepared from 5 wt % **1a**/cyclohexane gel, which indicated the formation of two-dimensional supramolecular assemblies instead of fibrous assemblies.[31] The XRD pattern of this xerogel (Fig. 8a) showed a strong peak at 1.94 nm, but other peaks were not clearly identified. As shown in Figure 8b and c, the xerogel of **1b** and **1c** prepared from their 5 wt % cyclohexane gels also showed similar peaks in the small-angle region, but their peak positions were shifted to the lower-angle side as the size of the alkylsilyl group increased. In the XRD patterns of **1b** and **1c**, broad and very weak peaks corresponding to the higher-order diffraction were observed, and no additional peak that can be assigned as a two-dimensional lattice was identified at all. Therefore, the results are in good agreement with the SEM observation, indicating the lamella-like layered structure in the xerogel.

The supramolecular assemblies of the **1a**/dodecane gel were directly observed by AFM after transferring onto a silicon wafer (Fig. 9). Though a fiber-like picture was obtained, a depth profile of the image indicated the two-dimensional layer structure. The size of the layer structure is 30–50 nm in width and 2.1 ± 0.3 nm in height, and this observed height is in good agreement with the observed spacing in the XRD measurement.

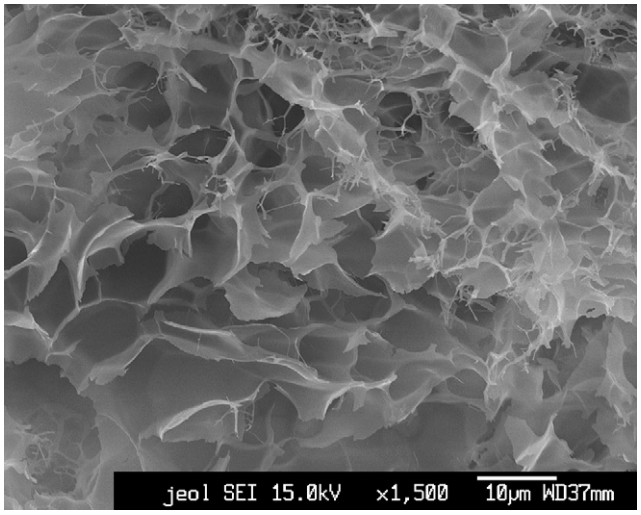

Figure 7. SEM image of the xerogel prepared from the **1a**/cyclohexane gel (5 wt %).

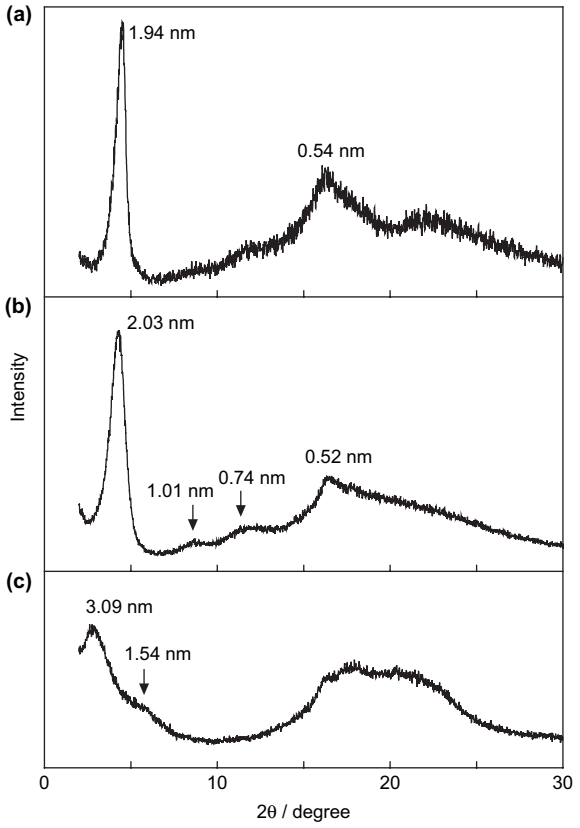

Figure 8. XRD patterns of the xerogels prepared from (a) **1a**, (b) **1b**, and (c) **1c** cyclohexane gels (5 wt %).

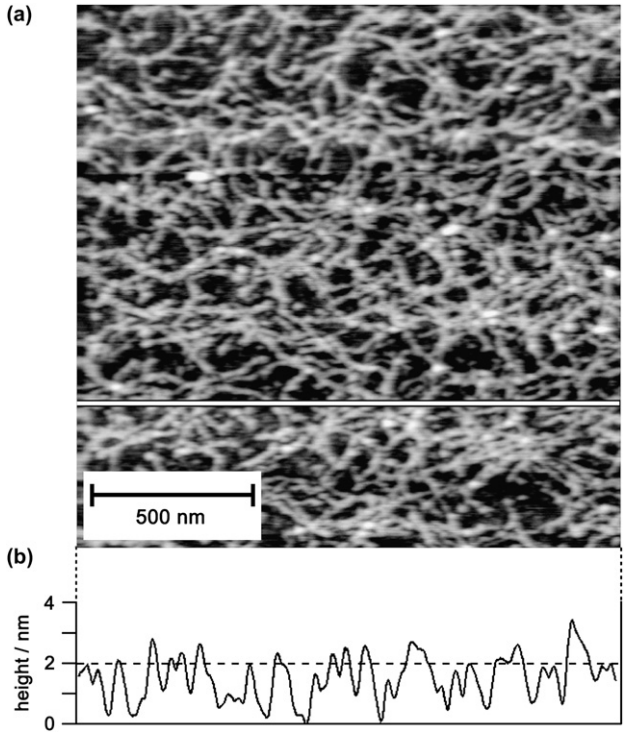

Figure 9. (a) AFM image of **1a**/dodecane gel (5 wt %) transferred onto a silicon substrate and (b) depth profile along the line in the image.

3. Discussion

3.1. G–G base pair formation

Hydrogen-bonded nucleobase pairs have been the subject of intense studies because of their critical role in information storage and processing of living organisms. Since nucleobases have multiple hydrogen bond donor and acceptor sites within their structure, a variety of hydrogen bonding patterns, including self-complementary base pairs, can be formed. In this study, the hydrogen bonding pattern of the guanine moiety in the gel was indicated to be a self-complementary G–G base pair by the formation of double N(2)H···N(3) hydrogen bonds (Fig. 5). From the point of view of the hydrogen bonding interaction, however, this G–G base pair does not seem to have sufficient stability to explain its selective formation. As to the guanine base, several different self-complementary base pairs formed by a double hydrogen bonding interaction have been discussed, in which hydrogen bonding at the C(6)=O position is mostly involved. Though this G–G base pair has been reported for parallel-stranded d(CpG), d(CpGpA), and d(TpCpGpA) duplexes in crystals and in solution at acidic pH,[27,28] base pair formation between C and C^+ (protonated C) rather than the G–G base pair formation was suggested to be the major driving force in these cases. Furthermore, an extensive ab initio calculation indicated that the interaction energy of this type of G–G base pair was much smaller than those of other self-complementary G–G base pairs formed by the hydrogen bonds at the C(6)=O position.[32] In the case of polymeric hydrogen bonding patterns like linear tapes and sheet (Fig. 1), an additional 2–3 hydrogen bonds, including C(6)=O and N(1)H, were formed and, therefore, formation of these polymeric hydrogen bonding networks should be thermodynamically favored. However, the sharp C(6)=O peak observed at 1718 cm^{-1} (Fig. 4a) clearly indicated the absence of the hydrogen bonding interaction at this position, excluding the formation of other self-complementary base pairs or polymeric hydrogen bonding networks. Therefore, the formation of this G–G base pair cannot be explained simply by the hydrogen bonding interactions, although additional hydrogen bonding interaction with 2′-O may contribute to some extent to the stability of this base pair.

To understand the G–G base pair in more detail, we examined its structure by a semi-empirical calculation (MOPAC PM3), and the optimized structure is shown in Figure 10. Since this level of calculation is insufficient to discuss the

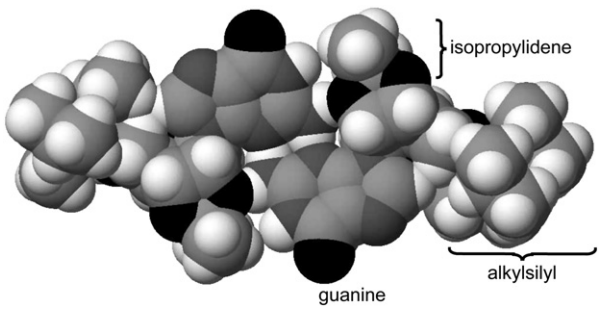

Figure 10. The G–G base pair model optimized by MOPAC PM3.

interaction energy,[32] we discuss only the structural aspect of the base pair. The hydrogen bond distances are 0.184 nm for N(2)H···N(3) (∠NHN=167°) and 0.186 nm for N(2)H···O(2′) (∠NHO=159°), which are sufficiently short for the hydrogen bond distance. In the optimized structure, the methyl group of the isopropylidene moiety came close to the N(1)H hydrogen atom, which might interfere with the hydrogen bonding interaction at this position. However, examination of other hydrogen bonding patterns of **1a**, including the G–G base pairs and tapes I and II, revealed that these hydrogen bonding patterns could be formed without serious steric hindrance even in the presence of the isopropylidene unit and the bulky alkylsilyl group at the 5′-position. Therefore, these discussions suggest that the hydrogen bond interaction is not the determining factor of the observed G–G base pair formation shown in Figure 5. It is interesting to note that Gottarelli and his group showed that the 5′-ester derivative of 2′,3′-isopropylidene guanosine induced gelation of organic solvents by the formation of tapes.[18] Therefore, the presence of the bulky alkylsilyl group at the 5′-position may be the essential factor for the formation of the G–G base pair.

Among the alkylsilylated guanosine derivatives we tested,[19–22] G–G base pair formation was observed only for **1a–c**. Therefore, the isopropylidene unit is also essential for the formation of this base pair. Since the bulky alkylsilyl and rigid isopropylidene-ribose moieties must be strongly demanding factors for the molecular packing within the self-assemblies, the molecular packing rather than stabilization by the hydrogen bonding interaction is suggested to play the critical role in determining the hydrogen bonding pattern.

This view is further supported by the thermal properties of the gel. Temperature-controlled IR spectra of the **1a**/dodecane gel clearly indicated that the hydrogen bond formation at the C(6)═O position was allowed only after heating above the gel-to-sol transition. Therefore, the molecular packing of the base pairs is the determining factor of the structure in the gel state. Interestingly, the sol–gel transition is reversible, showing that the gel structure is the thermodynamically favored state.

3.2. Structures of the supramolecular assemblies

XRD and SEM studies of the **1a** xerogel and AFM observation of the transferred gel indicated formation of a two-dimensional supramolecular assembly approximately 2 nm in height. Based on these results, a possible model structure of G–G base pair assembly is shown in Figure 11. Though no definitive evidence to determine the structure of the assembly has yet been obtained, this tentative model does not show any serious steric problem by a molecular mechanics calculation. Since the Si–Si distance in the base pair is 1.96 nm (Fig. 10), the alkyl chains in the structure might be highly tilted and/or partly interdigitated to become a lamella-like layered structure (Fig. 11).

In the case of molecular crystals, tight molecular packing is regarded to be the key determining factor of the crystal structure, which is known as Kitaigorodskii's close-packing principle.[33] The two-dimensional supramolecular assembly on the nano- to mesoscopic-scale does not seem to have a crystal-like organized structure from XRD, SEM, and AFM studies. However, the molecular assemblies of low molecular mass gelator **1a** within the soft gel might have a closely packed structure with sufficient rigidity to make molecular packing the key determining factor, which may be the reason for the low minimum gelation concentration. It is worth noting that the nucleation and development of the self-assemblies of low molecular mass gelators are frequently discussed from a crystal growth model.[34]

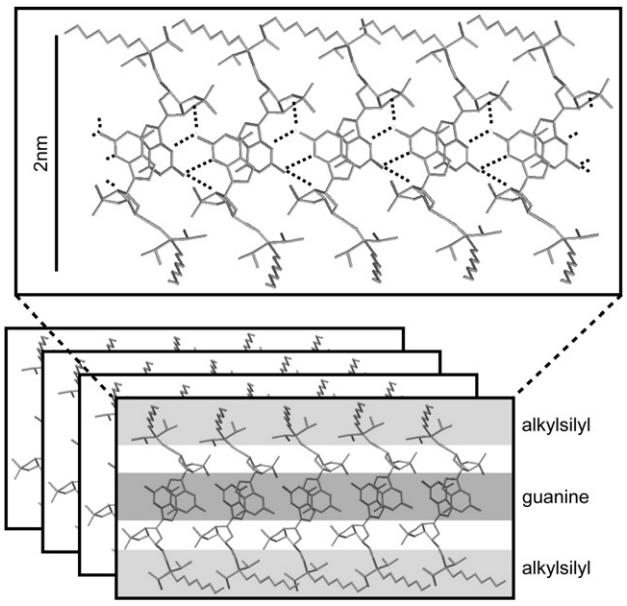

Figure 11. A model of the molecular assemblies in the **1a** gel optimized by a molecular mechanics calculation.

4. Conclusion

In summary, we designed and synthesized guanosine-based gelators **1a–c** having 2′,3′-*O*-isopropylideneribose and bulky alkylsilyl moieties, which showed excellent gelation ability in alkane solvents (minimum gelation concentrations 0.4–0.9 wt %). The absence of the hydrogen bonding interaction at the C(6)═O position and other evidence indicated the formation of the self-complementary G–G base pair through double N(2)H···N(3) hydrogen bonds within the gel, which further developed into the two-dimensional supramolecular assemblies approximately 2 nm in thickness and 30–50 nm in width. The determining factor of this G–G base pair formation and, hence, the structure of the supramolecular assembly, is suggested to be the molecular packing within the two-dimensional assemblies rather than the hydrogen bonding interaction.

5. Experimental

5.1. Measurements

A Perkin Elmer Pyris 1 DSC equipped with an Intracooler 2P was used for the DSC measurements. IR spectra were measured on a Shimadzu FTIR-8700 spectrometer attached to

a Spectra-Tech HT32 temperature-controlled liquid cell (room temperature–120 °C). Electronic absorption and circular dichroism (CD) spectra were measured by Shimadzu UV-2500PC and JASCO J-725 spectrometers, respectively. XRD measurements were operated on a Rigaku RINT-2100 diffractometer (Cu Kα) in the range of $2<2\theta<30°$. For AFM measurements, silicon wafers were pressed onto gel surfaces, and the transferred gel samples were subjected to tapping mode AFM observation using a JEOL JSPM-4200. ^{1}H NMR spectra were recorded on a JEOL AL400 spectrometer operated at 400 MHz. FABMS measurements were performed on a JEOL JMS-600H using glycerol as the matrix. For analysis, a Fisons Instruments EA1108 elemental analyzer was used. For the SEM measurement, a xerogel sample was shielded by a JEOL JFC-1600 auto fine coater equipped with an Au–Pd target, and the picture was obtained by a JEOL JSM-6330.

5.2. Modeling

Modeling was performed using CAChe™ version 6.01 (Fujitsu Ltd.). The MM3 parameter set was used for the molecular mechanics simulation, and the semi-empirical calculation was performed using MOPAC PM3.

5.3. Reagents

The reagents were purchased from Sigma–Aldrich Co., Tokyo Chemical Industry Co., and Wako Pure Chemical Industries, and were used without further purification. The solvents were dehydrated and distilled by routine procedures when necessary.

5.4. Synthesis

5.4.1. General procedure for alkylsilylation of nucleosides. Compounds **1a–c** and **2** were synthesized according to the method of Ogilvie et al.[23] A mixture of isopropylidene-nucleoside, chlorotrialkylsilane, and imidazole in the molar ratio of 1:2:5 in DMF (3 ml for 1 mmol of nucleoside) was stirred overnight at room temperature under an N_2 atmosphere. Chloroform was poured into the mixture and washed three times with water. The organic layer was dried by Na_2SO_4 and concentrated under reduced pressure. The crude residue was purified by silica gel column chromatography (Merck silica gel 60, chloroform/methanol=40:1–9:1). Compounds **1a–c** were further purified by precipitating from acetone.

Since chlorodiisobutyloctylsilane used for the synthesis of **1b** was not commercially available, this was synthesized according to the following procedure and was used immediately after preparation because of its high moisture sensitivity. To magnesium (turning, 7.54 g, 0.310 mol) in THF (50 ml), a solution of 1-bromo-2-methylpropane (1 ml, 0.009 mol) in THF (10 ml) was added dropwise and stirred for 30 min at room temperature under an N_2 atmosphere. 1-Bromo-2-methylpropane (32 ml, 0.294 mol) in THF (40 ml) was further added and stirred for 2 h. To the mixture, octyltrichlorosilane (30.7 ml, 0.133 mol) in THF (35 ml) was added dropwise and refluxed overnight. Removal of THF and subsequent vacuum distillation gave chlorodiisobutyloctylsilane (11.6 g, 0.040 mol). Yield: 30%. Bp: 125–128 °C (1.5 mmHg). ^{1}H NMR ($CDCl_3$) δ 0.45–0.60 (m, 6H, Si–CH_2–), 0.75–0.95 (m, 15H, –CH_3 (*i*-Bu, octyl)), 1.20–1.40 (m, 12H, –CH_2–), 1.80 (m, 4H, Me_2CH–). ^{13}C NMR ($CDCl_3$) δ 33.3, 32.0, 29.3, 29.2, 27.2, 26.2, 26.1, 24.5, 23.1, 22.7, 17.9, 14.2. IR (NaCl) 2955, 2926, 2856, 1463, 1398, 1381, 1366, 1331, 1221, 1165, 1094, 1040, 833, 775, 756, 669 cm^{-1}.

5.4.1.1. 2′,3′-*O*-Isopropylidene-5′-*O*-diisopropyloctylsilylguanosine (1a). Yield: 39%, white powder. Mp: 199.5–201.7 °C. R_f (silica gel, chloroform/methanol=9:1) 0.40. FABMS calcd for $C_{27}H_{48}N_5O_5Si_1$ [MH$^+$]: 550.34, found: 550.53. ^{1}H NMR ($CDCl_3$) δ 0.58–0.64 (m, 2H, Si–CH_2–), 0.83 (t, J=6.8 Hz, 3H, –CH_3 (octyl)), 0.9–1.0 (m, 14H, *i*-Pr), 1.1–1.3 (m, 12H, –CH_2– (octyl)), 1.37 (s, 3H, –CH_3 (isopropylidene)), 1.59 (s, 3H, –CH_3 (isopropylidene)), 3.81 (m, 2H, H(5′)), 4.30 (m, 1H, H(4′)), 4.93 (dd, J=3.0, 6.0 Hz, 1H, H(3′)), 5.12 (dd, J=2.4, 6 Hz, 1H, H(2′)), 5.99 (d, J=2.4 Hz, 1H, H(1′)), 6.22 (br, 2H, –NH_2(2)), 7.71 (s, 1H, H(8)), 12.03 (br, 1H, NH(1)). Analysis calcd (%) for $C_{27}H_{47}N_5O_5Si_1$ (549.78): C, 58.99, H, 8.62, N, 12.74, found: C, 59.00, H, 8.81, N, 12.63.

5.4.1.2. 2′,3′-*O*-Isopropylidene-5′-*O*-diisobutyloctylsilylguanosine (1b). Yield: 49%, white powder. A phase transition to a mesophase was observed at 194 °C, and melted to an isotropic liquid at 209 °C. R_f (silica gel, chloroform/methanol=9:1) 0.36. FABMS calcd for $C_{29}H_{52}N_5O_5Si_1$ [MH$^+$]: 578.37, found: 578.71. ^{1}H NMR ($CDCl_3$) δ 0.55–0.65 (m, 6H, Si–CH_2–), 0.8–0.95 (m, 15H, –CH_3 (*i*-Bu, octyl)), 1.2–1.3 (m, 12H, –CH_2– (octyl)), 1.37 (s, 3H, –CH_3 (isopropylidene)), 1.60 (s, 3H, –CH_3 (isopropylidene)), 1.76 (m, 2H, –$CHMe_2$), 3.75 (m, 2H, H(5′)), 4.30 (m, 1H, H(4′)), 4.89 (dd, J=2.8, 6.0 Hz, 1H, H(3′)), 5.09 (dd, J=2.8, 6.0 Hz, 1H, H(2′)), 5.95 (br, 2H, –NH_2(2)), 5.98 (d, J=2.8 Hz, 1H, H(1′)), 7.69 (s, 1H, H(8)), 12.08 (br, 1H, NH(1)). Analysis calcd (%) for $C_{29}H_{51}N_5O_5Si_1$ (577.83): C, 60.28, H, 8.90, N, 12.12, found: C, 60.07, H, 8.87, N, 11.82.

5.4.1.3. 2′,3′-*O*-Isopropylidene-5′-*O*-diisobutyloctadecylsilylguanosine (1c). Yield: 59%, white powder. Mp: 179.2–181.5 °C. R_f (silica gel, chloroform/methanol=9:1) 0.42. FABMS calcd for $C_{39}H_{72}N_5O_5Si_1$ [MH$^+$]: 718.53, found: 718.75. ^{1}H NMR ($CDCl_3$) δ 0.55–0.65 (m, 6H, Si–CH_2–), 0.8–0.95 (m, 15H, –CH_3 (*i*-Bu, octadecyl)), 1.1–1.3 (m, 32H, –CH_2– (octadecyl)), 1.36 (s, 3H, –CH_3 (isopropylidene)), 1.60 (s, 3H, –CH_3 (isopropylidene)), 1.76 (m, 2H, –$CHMe_2$), 3.75 (m, 2H, H(5′)), 4.30 (m, 1H, H(4′)), 4.89 (dd, J=3.2, 6.4 Hz, 1H, H(3′)), 5.08 (dd, J=2.8, 6.4 Hz, 1H, H(2′)), 5.92 (br, 2H, –NH_2(2)), 5.98 (d, J=2.8 Hz, 1H, H(1′)), 7.69 (s, 1H, H(8)), 12.11 (br, 1H, NH(1)). Analysis calcd (%) for $C_{39}H_{71}N_5O_5Si_1$ (718.10): C, 65.23, H, 9.97, N, 9.75, found: C, 65.40, H, 10.25, N, 9.60.

5.4.1.4. 2′,3′-*O*-Isopropylidene-5′-*O*-diisopropyloctylsilylcytidine (2). Yield: 39%, colorless hard gum. Mp: 92.0–93.6 °C. R_f (silica gel, chloroform/methanol=9:1) 0.44. FABMS calcd for $C_{26}H_{48}N_3O_5Si_1$ [MH$^+$]: 510.34, found: 510.54. ^{1}H NMR ($CDCl_3$) δ 0.6–0.69 (m, 2H, Si–CH_2–), 0.85 (t, J=6.8 Hz, 3H, –CH_3 (octyl)), 0.95–1.05 (m, 14H, *i*-Pr), 1.2–1.4 (m, 15H, –CH_2– (octyl), –CH_3

(isopropylidene)), 1.55 (s, 3H, $-CH_3$ (isopropylidene)), 3.81 (dd, J=4.0, 11 Hz, 1H, H(3′)), 3.94 (dd, J=2.4, 11 Hz, 1H, H(2′)), 4.25 (m, 1H, H(4′)), 4.74 (m, 2H, H(5′)), 5.60 (d, J=7.2 Hz, 1H, H(5)), 5.91 (d, J=2.4 Hz, 1H, H(1′)), 7.71 (d, J=7.2 Hz, 1H, H(6)). Analysis calcd (%) for $C_{26}H_{47}N_3O_5Si_1$ (509.75): C, 61.26, H, 9.29, N, 8.24, found: C, 60.99, H, 9.53, N, 8.43.

5.4.2. Synthesis of 2′-*O*-diisopropyloctylsilyl-3′,5′-*O*-di-*tert*-butylsilanediylguanosine (3). 3′,5′-*O*-(Di-*tert*-butylsilanediyl)guanosine was obtained according to the method of Furusawa et al.[24] To a mixture of 3′,5′-*O*-di-*tert*-butylsilanediylguanosine (0.478 g, 1.13 mmol), silver trifluoromethanesulfonate (0.726 g, 2.83 mmol), and dimethylformamide (10 ml), chlorodiisopropyloctylsilane (0.735 g, 2.80 mmol) was added and stirred for 10 min at room temperature under an N_2 atmosphere. After adding triethylamine (0.284 g, 2.81 mmol), the mixture was concentrated under reduced pressure. The crude residue was purified by silica gel column chromatography (Merck silica gel 60, chloroform/methanol=30:1) to give **3** (0.376 g, 0.578 mmol). Yield: 51%, white powder. Mp: 208.0–210.9 °C. R_f (silica gel, chloroform/methanol=9:1) 0.48. FABMS calcd for $C_{32}H_{60}N_5O_5Si_2$ [MH^+]: 650.41, found: 650.47. ^{1}H NMR ($CDCl_3$): δ: 0.65–0.71 (m, 2H, Si–CH_2–), 0.83 (t, J=6.8 Hz, 3H, $-CH_3$ (octyl)), 0.9–1.1 (m, 32H, *t*-Bu, *i*-Pr), 1.15–1.4 (m, 12H, $-CH_2-$ (octyl)), 3.98 (t, J=10 Hz, 1H, sugar), 4.14 (m, 1H, sugar), 4.4–4.5 (m, 2H, sugar), 4.59 (d, J=4.8 Hz, 1H, sugar), 5.72 (s, 1H, H(1′)), 5.90 (br, 2H, $-NH_2$(2)), 7.48 (s, 1H, H(8)), 11.92 (br, 1H, NH(1)). Analysis calcd (%) for $C_{32}H_{59}N_5O_5Si_2$ (650.01): C, 59.13, H, 9.15, N, 10.77, found: C, 59.22, H, 9.32, N, 10.71.

Acknowledgements

This study was partly supported by a Grant-in-Aid for Scientific Research (No. 14350482) from the Ministry of Education, Culture, Sports, Science, and Technology (MEXT) of Japan.

References and notes

1. Terech, P.; Weiss, R. G. *Chem. Rev.* **1997**, *97*, 3133–3159.
2. Estroff, L. A.; Hamilton, A. D. *Chem. Rev.* **2004**, *104*, 1201–1217.
3. Sangeetha, N. M.; Maitra, U. *Chem. Soc. Rev.* **2005**, *34*, 821–836.
4. *Low Molecular Mass Gelators*; Fages, F., Ed.; Topics in Current Chemistry; Springer: Berlin, 2005; Vol. 256.
5. Saenger, W. *Principles of Nucleic Acid Structure*; Springer: Berlin, Heidelberg, New York, NY, 1984.
6. Araki, K.; Yoshikawa, I. *Top. Curr. Chem.* **2005**, *256*, 133–165.
7. Kennard, O.; Hunter, W. N. *Angew. Chem., Int. Ed. Engl.* **1991**, *30*, 1254–1277.
8. Davis, J. T. *Angew. Chem., Int. Ed.* **2004**, *43*, 668–698.
9. Forman, S. L.; Fettinger, J. C.; Pieraccini, S.; Gottarelli, G.; Davis, J. T. *J. Am. Chem. Soc.* **2000**, *122*, 4060–4067.
10. Cai, M.; Marlow, A. L.; Fettinger, J. C.; Fabris, D.; Haverlock, T. J.; Moyer, B. A.; Davis, J. T. *Angew. Chem., Int. Ed.* **2000**, *39*, 1283–1285.
11. Mascal, M.; Hext, N. M.; Warmuth, R.; Moore, M. H.; Turkenburg, J. P. *Angew. Chem., Int. Ed.* **1996**, *35*, 2204–2206.
12. Mande, S. S.; Seshadri, T. P.; Viswamitra, M. A. *Acta Crystallogr., Sect. C: Cryst. Struct. Commun.* **1988**, *44*, 912–914.
13. Mande, S. S.; Seshadri, T. P.; Viswamitra, M. A. *Acta Crystallogr., Sect. C: Cryst. Struct. Commun.* **1989**, *45*, 92–94.
14. Bolon, P. J.; Sells, T. B.; Nuesca, Z. M.; Purdy, D. F.; Nair, V. *Tetrahedron* **1994**, *50*, 7747–7764.
15. Sheldrick, W. S.; Morr, M. *Acta Crystallogr., Sect. B: Struct. Crystallogr. Cryst. Chem.* **1980**, *36*, 2328–2333.
16. Gottarelli, G.; Masiero, S.; Mezzina, E.; Spada, G. P.; Mariani, P.; Recanatini, M. *Helv. Chim. Acta* **1998**, *81*, 2078–2092.
17. Gottarelli, G.; Masiero, S.; Mezzina, E.; Pieraccini, S.; Rabe, J. P.; Samorí, P.; Spada, G. P. *Chem.—Eur. J.* **2000**, *6*, 3242–3248.
18. Giorgi, T.; Grepioni, F.; Manet, I.; Mariani, P.; Masiero, S.; Mezzina, E.; Pieraccini, S.; Saturni, L.; Spada, G. P.; Gottarelli, G. *Chem.—Eur. J.* **2002**, *8*, 2143–2152.
19. Araki, K.; Takasawa, R.; Yoshikawa, I. *Chem. Commun.* **2001**, 1826–1827.
20. Takasawa, R.; Yoshikawa, I.; Araki, K. *Org. Biomol. Chem.* **2004**, *2*, 1125–1132.
21. Yoshikawa, I.; Li, J.; Sakata, Y.; Araki, K. *Angew. Chem., Int. Ed.* **2004**, *43*, 100–103.
22. Sato, T.; Seko, M.; Takasawa, R.; Yoshikawa, I.; Araki, K. *J. Mater. Chem.* **2001**, *11*, 3018–3022.
23. Ogilvie, K. K.; Schifman, A. L.; Penney, C. L. *Can. J. Chem.* **1979**, *57*, 2230–2238.
24. Furusawa, K.; Ueno, K.; Katsura, T. *Chem. Lett.* **1990**, 97–100.
25. Hanabusa, K.; Miki, T.; Taguchi, Y.; Koyama, T.; Shirai, H. *J. Chem. Soc., Chem. Commun.* **1993**, 1382–1384.
26. Szczepaniak, K.; Szczesniak, M.; Szajda, W.; Person, W. B. *Can. J. Chem.* **1991**, *69*, 1705–1720.
27. Cruse, W. B. T.; Egert, E.; Kennard, O.; Sala, G. B.; Salisbury, S. A.; Viswamitra, M. A. *Biochemistry* **1983**, *22*, 1833–1839.
28. Wang, Y.; Patel, D. J. *J. Mol. Biol.* **1994**, *242*, 508–526.
29. Clark, L. B.; Tinoco, I., Jr. *J. Am. Chem. Soc.* **1965**, *87*, 11–15.
30. Ikehara, M.; Uesugi, S.; Yoshida, K. *Biochemistry* **1972**, *11*, 830–836.
31. Shirakawa, M.; Fujita, N.; Shimakoshi, H.; Hisaeda, Y.; Shinkai, S. *Tetrahedron* **2006**, *62*, 2016–2024.
32. Hobza, P.; Šponer, J. *Chem. Rev.* **1999**, *99*, 3247–3276.
33. Kitaigorodskii, A. I. *Organic Chemical Crystallography*; Consultants Bureau: New York, NY, 1961.
34. Liu, X. Y. *Top. Curr. Chem.* **2005**, *256*, 1–37.